Asian Journal of Chemistry; Vol. 24, No. 1 (2012), 269-272

ASIAN JOURNAL OF CHEMISTRY

www.asianjournalofchemistry.co.in

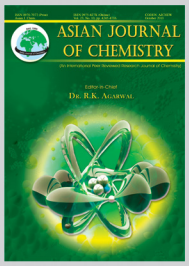

Quantum Chemical Calculations (QSAR) of Antipyrine Drug and Its Metabolites

AMMAR A. IBRAHIM[1,*], EID A. ABDALRAZAQ[2], MAHER A. IBRAHIM[3], ROSIYAH YAHYA[1] and ENTESAR A. SULLIMAN[4]

[1]Department of Chemistry, Faculty of Science, University of Malaya, 50603 Kuala Lumpur, Malaysia
[2]Department of Chemistry, College of Science, Al-Hussein Bin Talal University, Ma'an, Jordan
[3]Department of Biochemistry, College of Medicine, University of Mosul, Mosul, Iraq
[4]Department of Chemistry, College of Science, University of Mosul, Mosul, Iraq

*Corresponding author: E-mail: dr.ammar_1974@yahoo.com

(*Received*: 14 December 2010; *Accepted*: 15 September 2011) AJC-10415

The electronic properties of antipyrine and its metabolites have been investigated theoretically by the different methods of semi-empirical (AM1, MNDO/3 and PM3) and *ab initio* at STO-3G level calculations. These metabolites are of much interest due to their biological and medical importance. The charges, HOMO, LUMO, hardness (η), electronic chemical potential (μ) and global electrophilicity index (ω) were determined. The metabolites of A4 (according to MNDO/3) and A6 (according to AM1, PM3 and *ab initio*) have relatively low LUMO-HOMO differences indicating that these compounds would be the most reactive metabolites.

Key Words: Antipyrine, Metabolism, QSAR, Drug design, HOMO.

INTRODUCTION

The century ended with the development of the first of two synthesized drugs. The discovery of antipyrine in 1883 and aspirin in 1897 set the stage for the next 10 decades of the pharmaceutical century[1]. Phenyldimethyl-pyrazolone (or 2,3-dimethyl-1-phenyl-5-pyrazolone) (antipyrine), as its common name indicates, is an antipyretic, which means that it reduces the body temperature in fever. It exerts also a strong analgesic effect and is used as a sedative in disturbances accompanied by pain.

Studies of antipyrine metabolism may be used to illustrate the effect of inhibition on metabolism *in vivo*; persons exposed to DDT and lindane metabolized antipyrine twice as fast as a group not exposed, whereas those exposed to DDT alone had a reduced half-life for phenylbutazone and increased excretion of 6-hydroxycortisol[2].

Phenolic materials react with 4-aminoantipyrine at a pH of 10 to form a stable antipyrine dye. Direct photometric method is used when the phenol concentration in the effluent is high. Chloroform extraction method is used when the phenol concentration in the effluent is low[3].

Toropov and Mamaeva[4] had proposed a photometric determination of nitrate and nitrite ions using antipyrine in suphuric acid solutions. While Astakhina *et al.*[5] had determined aminoantipyrine in analgin product mixture by titration with sodium nitrite after the stages of boiling and HCl reduction. A new series of transition metal complexes of Cu(II), Ni(II), Co(II), Mn(II), Zn(II), VO(IV), Hg(II) and Cd(II) have been synthesized from the Schiff base (L) derived from 4-amino-antipyrine. Structural features were obtained from their elemental analyses, magnetic susceptibility, molar conductance, mass, IR, UV-VIS, ^{1}H NMR and ESR spectral studies[6].

The half-lives of antipyrine were studied in adult black patients and the values were observed about 5.7 ± 1.9 h. The antipyrine half-life was measured as an index of microsomal enzyme induction and the results showed a more rapid elimination of antipyrine (half-life 5.7 ± 1.9 h) in the patients under study than in those in most other published reports[7]. Complexes of some first row metal ions with ligands containing the antipyrine moiety N,N'-*bis*(4-antipyryl-methyl)-piperazine (BAMP) have also been studied[8-10].

Quantitative structure-activity relationship (QSAR) models have been developed for three pharmacological permeabilities, (log P_{app}) at different pH values of pH 5.5 and 7.4 and (log P_{app}(Caco-2))[11]. On the other hand, (QSAR) models were developed for blood-brain barrier and human serum albumin binding for a dataset of drugs where experimental values of both properties were available[12].

Welch *et al.*[13] accurately had determined the elimination half-life of antipyrine in rats by the serial determination of salivary antipyrine concentrations. It was necessary to administer 2 mg/kg of pilocarpine given to some rats in order to collect (by capillary tube) 5 mL of saliva per sample. Schiff

base ligands of 4-aminoantipyrine and substituted salicylaldehydes have also been synthesized and characterized using various spectroscopic techniques such as elemental analysis, UV-VIS, IR and NMR. Steric strain imposed by the methyl substitution on the 4-amino-antipyrine moiety of the Schiff base ligand, causing small change of the Cu(II) geometry, along with various weak interactions has been analyzed in detail[14].

Estimates of half-life and systemic clearance of antipyrine have been used for the *in vivo* assessment of hepatic drug oxidation in different species[15]. Owing to its low pK_a value and its small degree of plasma protein binding, antipyrine is distributed in total body water. New β-aminovinylketones with antipyrine moieties (LH) and their 3*d*-metal [Co(II), Ni(II), Cu(II), Zn(II)] chelates have been synthesized. Two types of chelates can be obtained based on the coordination of the (LH) ligand, depending when an available carbonyl (C=O) group of the antipyrine fragment is coordinated (M = Co, Ni) or not (M = Cu) to the metal center[16].

EXPERIMENTAL

The geometries of antipyrine and its metabolites (3-OH-methyl-antipyrine, 4,4'-dihydroxyantipyrine, 4'-OH-antipyrine, 4-OH-antipyrine, nor-antipyrine and 3-carboxyantipyrine) have been minimized using different level of quantum chemical calculations. AM1, PM3 and MNDO/3 methods have been used in the calculations with restricted Hartree-Fock (RHF) formalism at (0.1) RMS gradient using the (CS ChemOffice Ultra 6). The geometry of the compounds have been minimized by *ab initio* methods at STO-3G level. The minimization energy were carried out to give charges, HOMO, LUMO, hardness (η), electronic chemical potential (μ) and global electrophilicity index (ω).

RESULTS AND DISCUSSION

The structures of antipyrine and its metabolites (3-hydroxymethyl-antipyrine, nor-antipyrine, 4-hydroxy-antipyrine, 4'-hydroxy-antipyrine, 3-carboxy-antipyrine and 4,4'-dihydroxy-antipyrine) are shown in Fig. 1.

HOMO-LUMO energy separation ($\varepsilon_{LUMO-HOMO}$) can aid to clarify chemical reactivity and kinetic stability of the molecule. A molecule with a small HOMO-LUMO gap can be associated with a high chemical reactivity and low kinetic stability. Table-1 gives the theoretical calculations for all methods used in this study. (A4) has the lowest (LUMO-HOMO) energy difference (7.6800 eV as per MNDO/3) compared to (A6) (7.8440, 8.4890 and 11.5096 eV per AM1, PM3 and *ab initio* respectively), indicating that the metabolite of (A6) is most labile kinetically.

On the other hand, (A3) molecule is kinetically more stable than the others (8.2700 eV as per MNDO/3), (A4 has 8.5950 eV as per AM1), (A1 has 8.8770 and 12.8291 eV as per PM3 and *ab initio*). As for (A7), it has the largest negative value for the heat of formation suggesting that the metabolite may be stable thermodynamically.

Generally the charge of carbon atom has somewhat similar value irrespective of the different derivatives of the antipyrine ring (Fig. 2).

TABLE-1
CALCULATED THERMODYNAMIC PARAMETERS FOR ANTIPYRINE AND ITS METABOLITES

Molecule	Type of calculation	ε_{HOMO} (eV)	ε_{LUMO} (eV)	$\varepsilon_{LUMO-HOMO}$ (eV)	HF (kcal/mol)	μ	ω	η	Charge		
									C1	N2	N3
A2	MNDO/3	-7.9390	-0.0090	7.9300	-43.191	-3.9740	1.9915	3.9650	0.6233	-0.1307	0.0048
	AM1	-8.8140	-0.3690	8.4450	19.143	-4.5915	2.4964	4.2225	0.3138	-0.1963	-0.1051
	PM3	-9.1870	-0.4380	8.7490	-15.264	-4.8125	2.6472	4.3745	0.3031	-0.0384	0.0228
	STO-3G	-6.3487	6.2720	12.6206	–	-0.0384	0.0001	6.3103	–	–	–
A7	MNDO/3	-7.6340	0.0690	7.7030	-104.734	-3.7825	1.8574	3.8515	0.5336	-0.0927	-0.0386
	AM1	-8.6460	-0.2440	8.4020	-21.879	-4.4450	2.3516	4.2010	0.2955	-0.1809	-0.0923
	PM3	-8.8790	-0.2030	8.6760	-64.949	-4.5410	2.3767	4.3380	0.2858	-0.0159	0.0127
	STO-3G	-6.0012	6.4782	12.4794	–	0.2385	0.0046	6.2397	–	–	–
A5	MNDO/3	-7.8900	0.0770	7.9670	-54.490	-3.9065	1.9155	3.9835	0.6245	-0.1165	-0.0195
	AM1	-8.5190	-0.1880	8.3310	19.864	-4.3535	2.2750	4.1655	0.3137	-0.1913	-0.1173
	PM3	-8.9550	-0.1970	8.7580	-22.354	-4.5760	2.3909	4.3790	0.3055	-0.0372	0.0051
	STO-3G	-5.9392	6.5838	12.5230	–	0.3223	0.0083	6.2615	–	–	–
A4	MNDO/3	-7.6610	0.0190	7.6800	-47.131	-3.8210	1.9010	3.8400	0.5366	-0.1093	-0.0348
	AM1	-8.8320	-0.2370	8.5950	22.195	-4.5345	2.3923	4.2975	0.2983	-0.1881	-0.0893
	PM3	-8.9050	-0.2320	8.6730	-19.734	-4.5685	2.4065	4.3365	0.2874	-0.0202	0.0139
	STO-3G	-6.2524	6.4339	12.6862	–	0.0908	0.0006	6.3431	–	–	–
A1	MNDO/3	-7.9220	0.0270	7.9490	3.102	-3.9475	1.9603	3.9745	0.6276	-0.1329	-0.0153
	AM1	-8.7520	-0.1800	8.5720	63.767	-4.4660	2.3268	4.2860	0.3165	-0.1978	-0.1142
	PM3	-9.1000	-0.2230	8.8770	22.842	-4.6615	2.4479	4.4385	0.3072	-0.0410	0.0063
	STO-3G	-6.2818	6.5473	12.8291	–	0.1328	0.0014	6.4145	–	–	–
A3	MNDO/3	-7.9640	0.3060	8.2700	-13.370	-3.8290	1.7728	4.1350	0.6287	-0.1145	-0.0208
	AM1	-8.8670	-0.2830	8.5840	57.666	-4.5750	2.4383	4.2920	0.3168	-0.2129	-0.1361
	PM3	-9.1410	-0.2770	8.8640	24.326	-4.7090	2.5017	4.4320	0.3069	-0.0585	0.0304
	STO-3G	-6.3283	6.4698	12.7981	–	0.0707	0.0004	6.3990	–	–	–
A6	MNDO/3	-8.1810	-0.3390	7.8420	-90.101	-4.2600	2.3142	3.9210	0.6213	-0.1267	0.0146
	AM1	-9.0320	-1.1480	7.8840	-12.603	-5.0900	3.2862	3.9420	0.3070	-0.2008	-0.0777
	PM3	-9.3970	-0.9080	8.4890	-53.234	-5.1525	3.1274	4.2445	0.2943	-0.0365	0.0366
	STO-3G	-6.4722	5.0374	11.5096	–	-0.7174	0.0447	5.7548	–	–	–

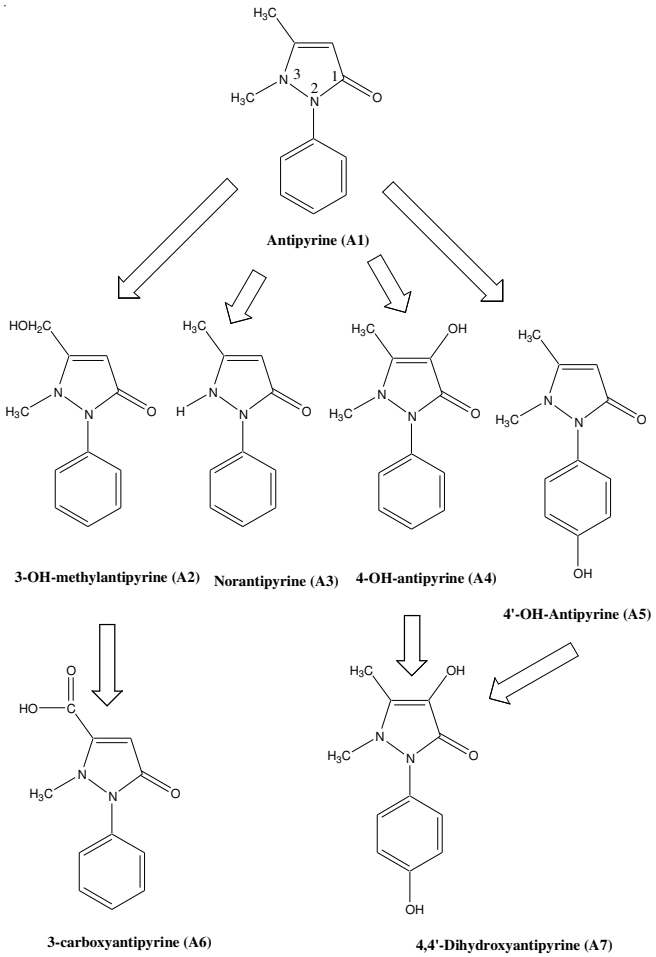

Fig. 1. Oxidative metabolic pathways for antipyrine drug

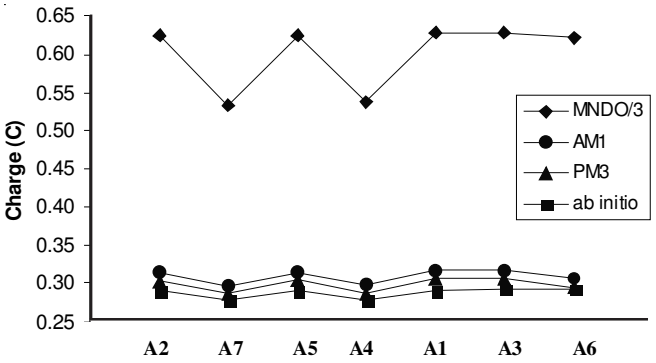

Fig. 2. Graph of carbon charge of antipyrine and its derivatives

MNDO/3, AM1, PM3 and *ab initio* calculations, all give similar behaviour of positive charge of carbon for each of the molecules except for (A4) and (A7). The reason of this exception is due to presence of the (OH) group from the carbon atom leading to donating more positive charge and delocalization of the charge in the ring.

Fig. 3 shows that the charge of nitrogen (N2) is more negative (less positive charge) for (A3) compound using (AM1 and PM3) due to the active group (CH_3) being replaced by (H) in the ring; while (A7) compound (MNDO/3, AM1 and PM3) has less negative charge (more positive charge) because there are many donor groups present which can increase the positive charge and decrease the negative charge.

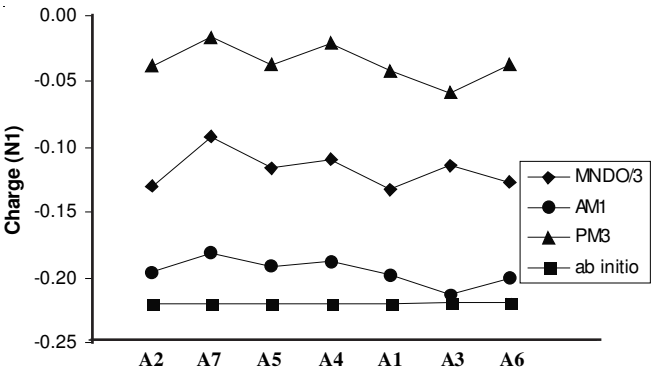

Fig. 3. Graph of nitrogen charge (N2) of antipyrine and its derivatives

From Fig. 4, (A6) compound has less negative charge (more positive charge) (AM1, PM3 and *ab initio*) because of the effect of the donor group (CH_3) being more effective than the acceptor group (COOH).

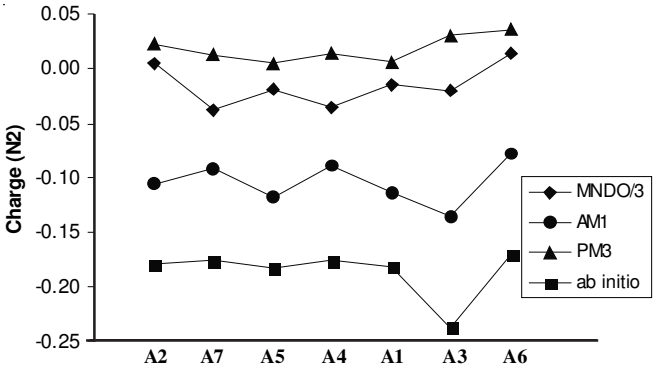

Fig. 4. Graph of nitrogen charge (N3) of antipyrine and its derivatives

Fig. 5 shows that (A6) compound has the lowest value of (LUMO-HOMO) gap (AM1, PM3 and *ab initio*), meaning that (A6) has the lowest absorbance value. The reason for this could be due to presence of the carboxylic acid which as an acceptor group can lead to decrease in the charge density in the benzene ring, thus decreasing the energy requirement to remove (oxidation) or accept (reduction) the electron in the orbital energy.

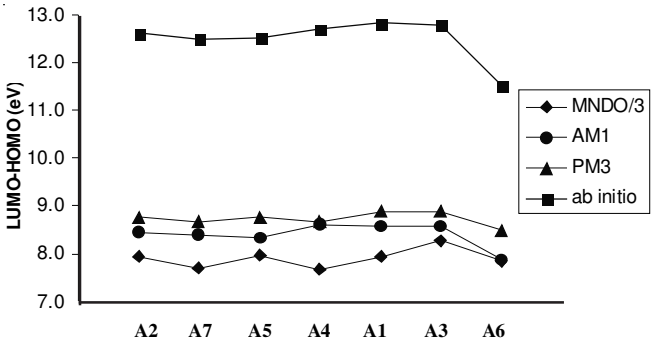

Fig. 5. Graph of (LUMO-HOMO) gap of antipyrine and its derivatives

Conclusion

There are limited studies in the literature about the molecules considered in this work. The results of such theoretical

work will aid in the elucidation of structure activity relationships of compounds in drugs before they can be safely evaluated and commercially developed as beneficial pharmaceuticals.

The geometry of antipyrine and its metabolites have been minimized based on semi-empirical (AM1, MNDO/3 and PM3) and *ab initio* calculations at STO-3G level.

REFERENCES

1. M.S. Lesney, Patents and Potions: Entering the Pharmaceutical Century, The Pharmaceutical Century: Ten decades of Drug Discovery Supplement to American Chemical Society, pp. 18-31 (2000).
2. H. Ernest, A Textbook of Modern Toxicology, John Wiley & Sons, Inc. Publication, edn. 3 (2004).
3. K.B. Nayana, Project Report, Treatement of Industrial Effluents in A Bioreactor, National Institute of Technology, Rourkela, India (2009).
4. L.I. Toropov and N.A. Mamaeva, *J. Anal. Chem.*, **54**, 529 (1999).
5. N.S. Astakhina, Z.I. Eremina and N.I. Sitak, *Khim. Farmatsevt. Zh.*, **11**, 126 (1997).
6. N. Raman, R.J. Dhaveethu and A. Sakthivel, *J. Chem. Sci.*, **119**, 303 (2007).
7. N. Buchanan, P. Bill, G. Moodley and C. Eyberg, *S. Afr. Med. J.*, **52**, 394 (1977).
8. O. Costisor, A. Maurer, A. Tomescu and P. Policec, *Bul. St. Tehn. Inst. Pol., Timisoara, Ser. Chim.*, **26**, 93 (1981).
9. O. Costisor, W. Linert, S. Deusch and C. Stanescu, *J. Coord. Chem.*, **33**, 229 (1994).
10. W. Linert, O. Costisor and R. Tudose, *Orient. J. Chem.*, **11**, 107 (1995).
11. K. Mati, K. Gunnar, T. Tarmo, T. Indrek, J. Jaak, T. Kaido, L. Andre, S. Deniss and D. Dimitar, *Arkivoc*, 218 (2009).
12. K. Mati, D. Dimitar, T. Tarmo, T. Indrek, J. Jaak, T. Kaido, L. Andre, S. Deniss and K. Gunnar, *Arkivoc*, 38 (2008).
13. R.M. Welch, R.L. DeAngelis, M. Wingfield and T.W. Farmer, *Clin. Pharmacol. Therapeut.*, **18**, 249 (1975).
14. S.P. Mosae, E. Suresh and P.S. Subramanian, *Polyhedron*, **26**, 749 (2007).
15. P.K. Koning and L. Cantilena, *Ann. Int. Med.*, **154**, 590 (1994).
16. A.D. Garnovskii, I.K. Boris, E.L. Anpilova, A.V. Bicherov, O.Yu Korshunov, A.S. Burlov, A.M. Miguel, L.M. Blanco, G.S. Borodkin, I.E. Uflyand and U.O. Mendez, *Polyhedron*, **23**, 1909 (2004).